JACS
JOURNAL OF THE AMERICAN CHEMICAL SOCIETY
Article
Cite This: J. Am. Chem. Soc. 2018, 140, 16488−16494
pubs.acs.org/JACS

Synthesis and Characterization of *cyclo*-Pentazolate Salts of NH_4^+, NH_3OH^+, $N_2H_5^+$, $C(NH_2)_3^+$, and $N(CH_3)_4^+$

Chen Yang,[†,⊥] Chong Zhang,[†,⊥] Zhansheng Zheng,[†] Chao Jiang,[†] Jun Luo,[†] Yang Du,[†] Bingcheng Hu,[*,†] Chengguo Sun,[*,†,‡] and Karl O. Christe[†,§]

[†]School of Chemical Engineering, Nanjing University of Science and Technology, Nanjing, Jiangsu 210094, China
[‡]School of Chemical Engineering, University of Science and Technology Liaoning, Anshan, Liaoning 114051, China
[§]Loker Hydrocarbon Research Institute and Department of Chemistry, University of Southern California, Los Angeles, California 90089-1661, United States

Supporting Information

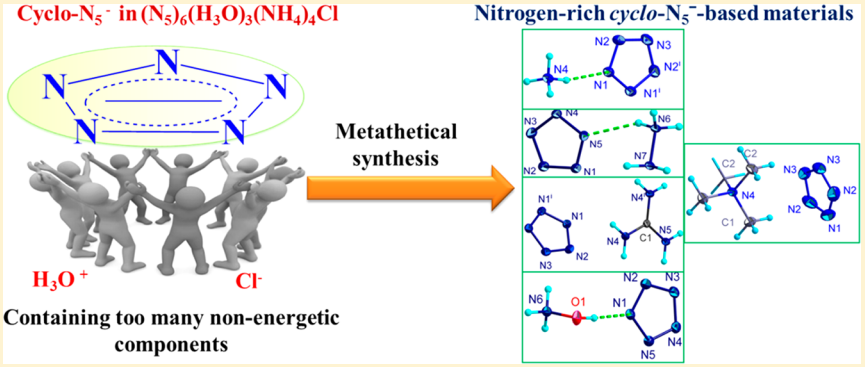

ABSTRACT: A breakthrough in polynitrogen chemistry was recently achieved by our bulk synthesis of $(N_5)_6(H_3O)_3(NH_4)_4Cl$ in which the *cyclo*-pentazolate anions were stabilized extensively by hydrogen bridges with the NH_4^+ and OH_3^+ cations. Significant efforts have been carried out to replace these nonenergetic cations and the Cl^- anion by more energetic cations. In this paper, the metathetical syntheses of *cyclo*-pentazolate salts containing the simple nitrogen-rich cations NH_4^+, NH_3OH^+, $N_2H_5^+$, $C(NH_2)_3^+$, and $N(CH_3)_4^+$ are reported. These salts were characterized by their crystal structures; vibrational, mass, and multinuclear NMR spectra; thermal stability measurements; sensitivity data; and performance calculations. It is shown that the *cyclo*-pentazolates are more energetic than the corresponding azides but are thermally less stable decomposing in the range of 80 °C to 105 °C. As explosives, the hydrazinium and hydroxyl ammonium salts are predicted to match the detonation pressure of RDX but exhibit significantly higher detonation velocities than RDX and HMX with comparable impact and friction sensitivities. Although the ammonium salt has a lower detonation pressure than RDX, its detonation velocity also exceeds those of RDX and HMX. As a rocket propellant, the hydrazinium and hydroxyl ammonium salts are predicted to exceed the performances of RDX and HMX. The crystal structures show that the *cyclo*-pentazolate anions are generally stabilized by hydrogen bonds to the cations, except for the $N(CH_3)_4^+$ salt which also exhibits strong cation-π interactions. This difference in the anion stabilization is also detectable in the vibrational spectra which show for the $N(CH_3)_4^+$ salt a decrease in the *cyclo*-N_5^- stretching vibrations of about 20 cm^{-1}.

1. INTRODUCTION

High-energy density materials (HEDMs) providing high energy release and green reaction products have been pursued for many years without much success.[1−6] However, polynitrogen compounds can meet these requirements because of their large positive heats of formation and the huge decomposition-energy release due to the highly exothermic formation of triply bonded dinitrogen.[7−9] No neutral room-temperature stable nitrogen allotropes and only three polynitrogen ions, N_3^-, N_5^+, and *cyclo*-N_5^-, had been known.[7,10] Whereas bulk syntheses had been available for N_3^- and N_5^+ salts for many years, for *cyclo*-N_5^- a bulk synthesis was discovered only during the past year by the isolation of $(N_5)_6(H_3O)_3(NH_4)_4Cl$.[11] In this compound, the *cyclo*-N_5^- anions were stabilized by strong hydrogen bonds to the NH_4^+ and OH_3^+ cations. Since these cations and the Cl^- anion are nonenergetic, subsequent work was focused on replacing them with simpler and/or more energetic cations. Some progress was made in this direction by the syntheses of $[M(H_2O)_4(N_5)_2]\cdot 4H_2O$ (M = metal cation) and simple metal *cyclo*-N_5^- salts (M = Na, Ag) in which the *cyclo*-N_5^- anions are stabilized by metal−nitrogen bonds.[12−19] Recently, the nitrogen-rich pentazolate salt $(NH_4)^+N_5^-$ has been predicted to

Received: May 15, 2018
Published: November 5, 2018

DOI: 10.1021/jacs.8b05106
J. Am. Chem. Soc. 2018, 140, 16488−16494

exist at high pressures above 30 GPa.[20] In this work, we report the syntheses of $M^+N_5^-$ salts in which M are simple, nitrogen-containing, and more energetic cations. The most common method to accomplish the exchange of ions in ionic compounds is metathesis. It requires the starting materials, A^+B^- and C^+D^- (eq 1), to be soluble and one of the desired products, AD or CB, to be insoluble to permit easy product separation.

$$A^+B^- + C^+D^- \rightarrow AD \downarrow + C^+B^- \quad (1)$$

In this manner, the *cyclo*-pentazolates of NH_4^+, NH_3OH^+, $N_2H_5^+$, $C(NH_2)_3^+$, and $N(CH_3)_4^+$ were prepared and fully characterized.

2. RESULTS AND DISCUSSION

2.1. Syntheses. Two different metathetical approaches were used in this study taking advantage of the low solubility of either AgI or $MgSO_4$ in CH_3OH/H_2O (Scheme 1). In both

Scheme 1. Metathetical Syntheses of the Different *cyclo*-Pentazolate Salts

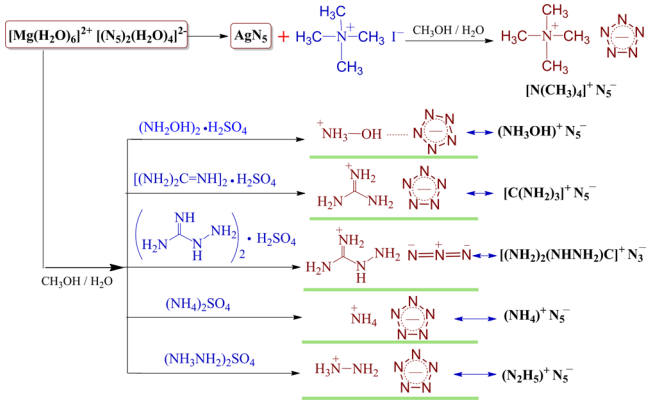

cases, the starting material was $[Mg(H_2O)_6]^{2+}[(N_5)_2(H_2O)_4]^{2-}$. For the synthesis of $[N(CH_3)_4]^+N_5^-$, the Mg salt was first converted to the poorly soluble AgN_5 salt and then further converted to the even less soluble AgI salt. For the remaining salts, the Mg starting material was reacted with the desired sulfates, and the resulting insoluble $MgSO_4$ was filtered off. Attempts to isolate the aminoguanidinium *cyclo*-pentazolate salt resulted in the corresponding azide due to the easy loss of N_2. In view of this easy loss of N_2 for aminoguanidine, we investigated the effect of other amines, such as methylamine (CH_3NH_2), pyridine (C_5H_5N), imidazole ($C_3H_4N_2$), and of triphenylphosphine (PPh_3) on the stability AgN_5 (Figure S1 of the Supporting Information, SI). When the amines and phosphine were added dropwise to an AgN_5 suspension in C_2H_5OH, the solid dissolved with N_2 evolution. The rate of N_2 evolution decreased in the order $CH_3NH_2 > C_3H_4N_2 \geq PPh_3 \geq C_5H_5N$. A few days after the CH_3NH_2 addition, the solution turned black and no signal of *cyclo*-N_5^- was detected by electrospray ionization (ESI) mass spectrometry (ESI−MS). The other solutions gave colorless single crystals that were characterized by single-crystal X-ray diffraction as $(PPh_3)_2Ag(N_3)_2Ag(PPh_3)_2$ and $(C_3H_3N_2)Ag(C_3H_3N_2)Ag$ (Figure 1A, B).

The silver atoms in $(PPh_3)_2Ag(N_3)_2Ag(PPh_3)_2$ are linked through a double azido (N_3^-) bridge and each silver atom is also coordinated to two P atoms from two triphenylphosphine molecules (Figure S29). The crystal structure of $(C_3H_3N_2)Ag(C_3H_3N_2)Ag$ exhibits linear chains running along the *b* axis involving the strong interactions between the Ag^+ cations and the anionic imidazolate groups (Figure S30). Although we failed to obtain a crystal structure for the pyridine adduct, the *cyclo*-N_5^- was still detected in the solid by ESI−MS (Figure S31). The azide ion (N_3^-) observed in $(PPh_3)_2Ag(N_3)_2Ag(PPh_3)_2$ suggests that the PPh_3 ligand partially breaks the pentazole ligand, resulting in the formation of N_3^- and N_2.

2.2. Crystal Structures of the *cyclo*-Pentazolates. All the structures of the *cyclo*-pentazolates were confirmed by single-crystal X-ray diffraction analysis, and complete crystal data can be found in the SI (Tables S1−S29). ORTEP views of the asymmetric units and atom labeling of hydroxylammonium *cyclo*-pentazolate, $(NH_3OH)^+N_5^-$, and guanidinium *cyclo*-pentazolate, $[C(NH_2)_3]^+N_5^-$, are given in Figure 1C, D. Hydrogen bonding acts as a determinant force to sustain the intricate architecture. In $(NH_3OH)^+N_5^-$, three of the four protons of the $(NH_3OH)^+$ cation can also act as three H-bond donor units for participation in hydrogen bonding with N1, N2, and N3 of *cyclo*-N_5^-(N(6)−H(6B)···N(3)$^{\#1}$, 2.8902(11) Å; N(6)−H(6C)···N(5)$^{\#2}$, 2.8744(11)Å; O(1)−H(1)···N(1), 2.7401(11) Å). Figure 2A shows a 2D diagram in which *cyclo*-N_5^- units are linked together to create the regular hydrogen bonding network. On the basis of the 2D network, the crystalline framework in 3D space can be constructed by extending the 2D layered structures (Figure 3A). Regarding the structure of $[C(NH_2)_3]^+N_5^-$, both the $[C(NH_2)_3]^+$ cation and *cyclo*-N_5^- anion are completely planar, and the guanidinium hydrogens were placed in the idealized positions.[21] All hydrogen bonds in $[C(NH_2)_3]^+N_5^-$ fall within the hydrogen-bond distance criterion, ranging in bond length from 3.0 to 3.4 Å, but deviate from linearity, with hydrogen bond angles ranging from 112.4° to 163.5°. Each individual pair of N−H···N interactions, shown in Figure 2B, can be characterized as a dimer formed via three amino protons on three nitrogen atoms of a single guanidinium ion and three lone electron pairs on three N atoms of a *cyclo*-N_5^- anion. Typical of the 3D framework, progressive increases in dimensionality are formed by hydrogen bonding (Figure 3B). As revealed by the unit cell structures, hydrogen bonding provides the major driving force for crystal packing and the stability of *cyclo*-N_5^- in both $[(NH_3OH)^+N_5^-]$ and $[C(NH_2)_3]^+N_5^-$ (Figures S32 and S33).

The tetramethylammonium *cyclo*-pentazolate, $[N(CH_3)_4]^+N_5^-$, was also successfully prepared. Its crystal structure is shown in Figure 1E. It crystallizes in the monoclinic space group $P2_1/m$ with two molecules per unit cell (Figure S34). Most frequently, *cyclo*-N_5^- acts as a hydrogen bond acceptor or prefers to form a coordinative bond with metal cations when forming stable pentazolate salts, although it has a conjugated π_5^6 bond. At first glance, we might suppose that either the weak hydrogen bonding or C−H···π interaction might be responsible for the stability of $[N(CH_3)_4]^+N_5^-$. To our best knowledge, the C−H···π interaction is not merely a conventional van der Waals force but has a hydrogen-bond-like property.[22] The most important geometrical characteristic of hydrogen bonds is that the distance between the proton and the acceptor atom is shorter than the sum of their van der Waals radii.[23] However, the C−H···N contacts with a distance of 2.7992 Å, are appreciably longer than the sum of the van der Waals radii (2.75) (Figure S35), suggesting that the hydrogen-bonding might be ignored for

DOI: 10.1021/jacs.8b05106
J. Am. Chem. Soc. 2018, 140, 16488−16494

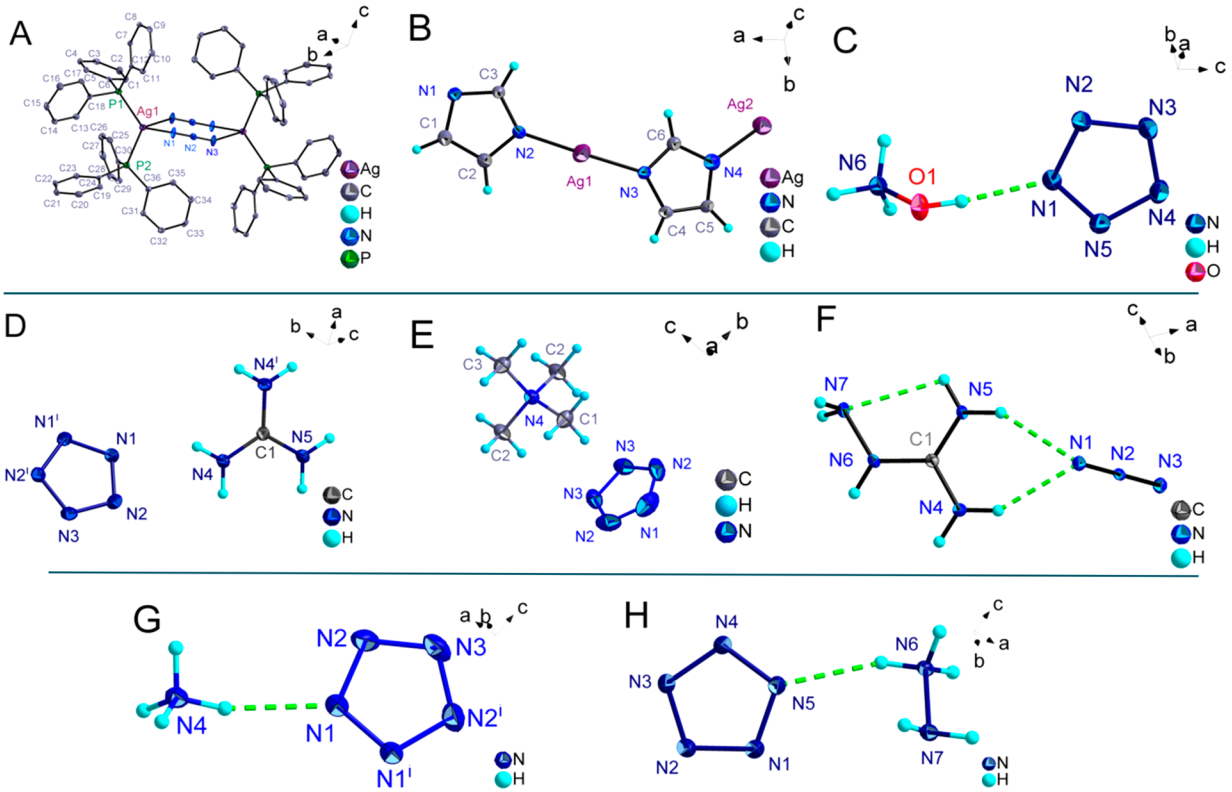

Figure 1. Ellipsoid plots of the synthesized crystals. (A) $(PPh_3)_2Ag(N_3)_2Ag(PPh_3)_2$; (B) $(C_3H_3N_2)Ag(C_3H_3N_2)Ag$; (C) $(NH_3OH)^+N_5^-$; (D) $[C(NH_2)_3]^+N_5^-$; (E) $[N(CH_3)_4]^+N_5^-$; (F) $[(NH_2)_2(NHNH_2)C]^+N_3^-$; and (G) $(NH_4)^+N_5^-$; (H) $(N_2H_5)^+N_5^-$.

explaining the stability of the tetramethylammonium salt. Under most circumstances, C−H···π interactions are weaker than classical chemical bonds, as evidenced by data that the binding energy of methane with the benzene ring, primarily attributed to dispersion, is only around 1.4 kcal/mol.[24] As a consequence, the lack of hydrogen bonding and coordination bonds in $[N(CH_3)_4]^+N_5^-$ may enhance the activity of the π system. Figure 2C shows an illustration of the cation-π interaction in which the binding of the $[N(CH_3)_4]^+$ cation to the π-face of *cyclo*-N_5^- is responsible for the overall crystal structure. The $[N(CH_3)_4]^+$ cation is located above the ring with an N−centroid distance of 4.2272(19) Å and a tilt angle of 76.389(162)°, but not exactly over the ring centroid. This situation is quite different from that observed for K^+/Na^+−π interactions, in which the alkali metal ions are usually located directly over the centroid with a tilt angle of 90°,[25] while the distribution occurs in the prevailing models of anion−π interactions.[26] Interestingly, $[N(CH_3)_4]^+N_5^-$ is the first example of a known *cyclo*-pentazolate compound in which cation−π interaction leads to higher stability.

In contrast to guanidinium sulfate, the aminoguanidinium cation $[(NH_2)_2(NHNH_2)C]^+$ while possessing a similar charge delocalization, is projected to form potentially more hydrogen bonding sites.[21] However, the steric hindrance and asymmetry of the terminal NH_2 group causes the decomposition of *cyclo*-N_5^- during the metathesis reaction, resulting in the aminoguanidinium azide, $[(NH_2)_2(NHNH_2)C]^+N_3^-$. Figures 1F and 2D show its crystal structure and the schematic representation of the hydrogen-bonded network between $[(NH_2)_2(NHNH_2)C]^+$ and N_3^-, in which all hydrogens participate in hydrogen bonding. Each N_3^- anion is surrounded by eight hydrogen bonds where six hydrogen bonds are equally assigned to the terminal nitrogens N1 and N3 of the isolated azide ions, while two hydrogen bonds involve the N2 atom. Apparently, the N_3^- anion is attracted by $[(NH_2)_2(NHNH_2)C]^+$, and are perfectly packed together by hydrogen-bonding (Figure S36). We expected that the replacement of *cyclo*-N_5^- by N_3^- would disturb the balance of the structure, and that it would be very hard to match the interaction forces between the two nearly planar ions due to the steric hindrance and asymmetry of the terminal NH_2 group. Thus, the forces acting on the ring of *cyclo*-N_5^- are not uniform, and this imbalance causes the decomposition of *cyclo*-N_5^- to N_3^-. To summarize the observed phenomenon, we conclude that the counterion used to pair with *cyclo*-N_5^- should be less steric hindering and be of high symmetry.

The crystal structures of $(NH_4)^+N_5^-$ and $(N_2H_5)^+N_5^-$ display interesting and similar molecular packing features involving strong hydrogen bonds and π−π interactions. In $(NH_4)^+N_5^-$, an axisymmetric structural motif R_4^4 (10) was generated by hydrogen bonds of N4−H4A···N1 and N4−H4B···N2 (Figures 1G and 2E). The interesting 3D hydrogen-bonded framework Figure 3C) is formed by the interlocked R_4^4 (10) motifs, which are linked by *cyclo*-N_5^- rings and expand along the [−120] and [120] directions, and the nearly perpendicular long chains are linked by NH_4^+. The interpenetrating networks are connected by π−π interaction among adjacent *cyclo*-N_5^- rings with centroid−centroid distances of 3.9137(7) Å (Figures 2F, S37, and S38). By replacing the NH_4^+ cation with $N_2H_5^+$, an extra H-bond donor (NH_2) becomes available. The 3D hydrogen-bonded framework (Figure 3D) can be interpreted as an interlaced net along the *c*-axis, that is interlocked by the R_4^4 (10) motif (Figures 1H and 2G), and a hydrogen-bonded dimer along the [110]

DOI: 10.1021/jacs.8b05106
J. Am. Chem. Soc. 2018, 140, 16488−16494

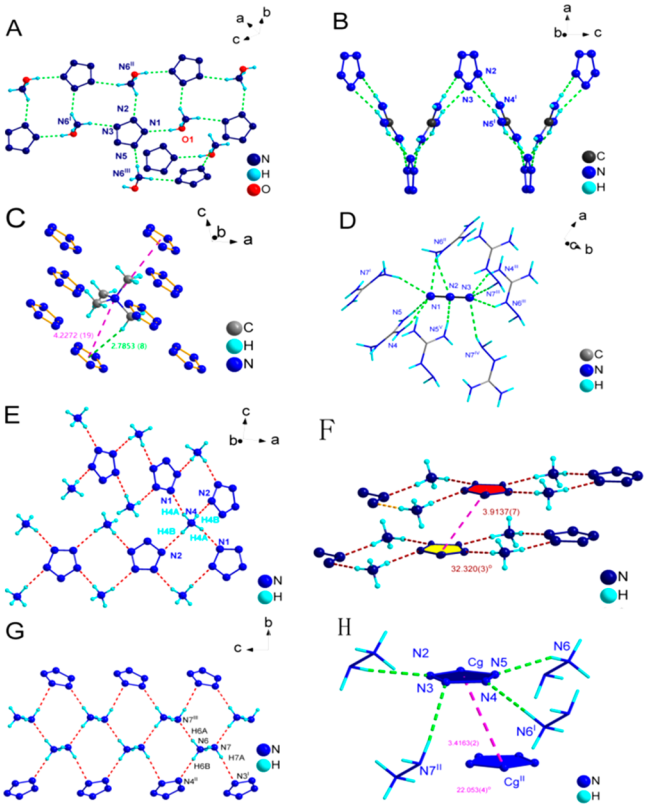

Figure 2. Schematic representation of the interionic forces motifs in the crystal structures. (A) Hydrogen-bonded motifs in $(NH_3OH)^+N_5^-$; (B) Hydrogen-bonded motifs in $[C(NH_2)_3]^+N_5^-$; (C) cation–π interactions in $[N(CH_3)_4]^+N_5^-$; (D) hydrogen-bonded motifs in $[(NH_2)_2(NHNH_2)C]^+N_3^-$; (E) hydrogen-bonded motifs in $(NH_4)^+N_5^-$; (F) π–π interactions in $(NH_4)^+N_5^-$; (G) hydrogen-bonded motifs in $(N_2H_5)^+N_5^-$; and (H) π–π interactions in $(N_2H_5)^+N_5^-$.

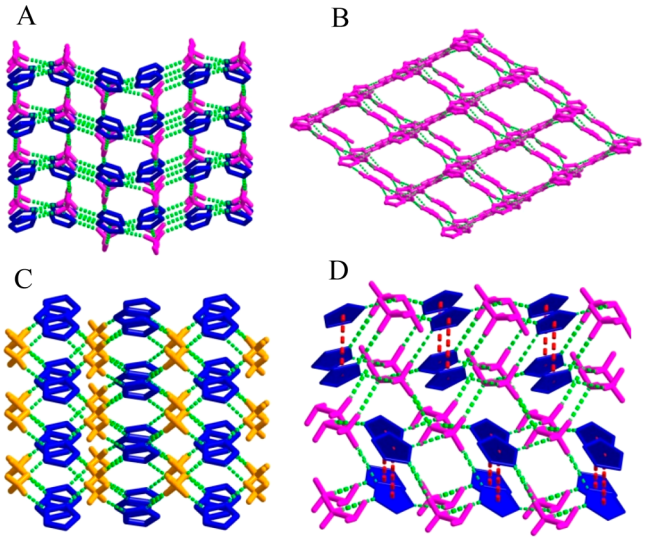

Figure 3. 3D crystalline framework. (A) $(NH_3OH)^+N_5^-$; (B) $[C(NH_2)_3]^+N_5^-$; (C) $(NH_4)^+N_5^-$; and (D) $(N_2H_5)^+N_5^-$.

direction, that is extended into an undulated ribbon involving a $C_2^2(7)$ motif (Figure S39). As with the 3D hydrogen-bonded framework of $(NH_4)^+N_5^-$, there is also an interpenetrating interlinkage of π–π interactions between the *cyclo*-N_5^- rings in $(N_2H_5)^+N_5^-$, and the π–π stacking provides a moderate interaction for the stabilization of the structure (Figures 2H, S40, and S41).

2.3. Thermal Behavior. Thermal stability remains a major concern for *cyclo*-N_5^--based compounds. The thermal behavior of five *cyclo*-pentazolate compounds, $(NH_3OH)^+N_5^-$, $[C(NH_2)_3]^+N_5^-$, $[N(CH_3)_4]^+N_5^-$, $(NH_4)^+N_5^-$ and $(N_2H_5)^+N_5^-$, were evaluated by thermogravimetry–differential scanning calorimetry–mass spectrometry–infrared spectroscopy (TG-DSC-MS-IR) at 5 °C min^{-1}. The DSC curves in Figure 4 indicate that they have the common feature that none of these compounds melts prior to decomposition.

Generally, the 3D plots of the FTIR spectra of evolved gases give important information on the thermal degradation of these compounds. As found in the simultaneously recorded IR spectra (Figure 4F–J), the evolution curves of the main gaseous products show that all pentazolate compounds first

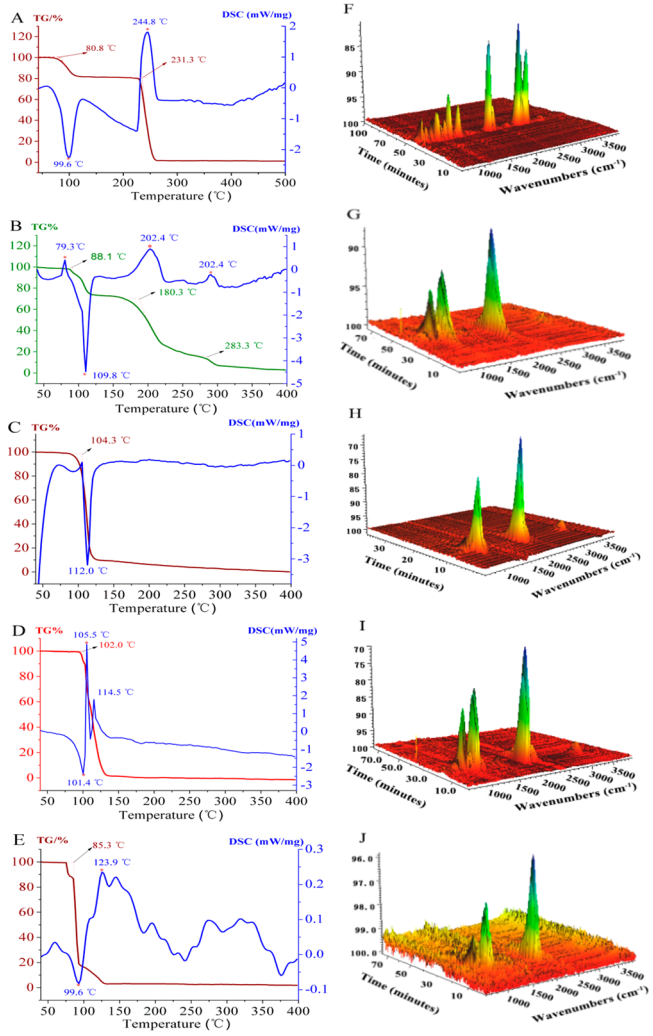

Figure 4. Thermal analysis of *cyclo*-pentazolate compounds under argon at 5 K/min and the IR spectra of the gaseous products obtained from their thermal decomposition. (A) TG-DSC curves of $[N(CH_3)_4]^+N_5^-$; (B) TG-DSC curves of $[C(NH_2)_3]^+N_5^-$; (C) TG-DSC curves of $(NH_3OH)^+N_5^-$; (D) TG-DSC curves of $(NH_4)^+N_5^-$; (E) TG-DSC curves of $(N_2H_5)^+N_5^-$; (F) IR spectrum of volatiles from $[N(CH_3)_4]^+N_5^-$; (G) IR spectrum of volatiles from $[C(NH_2)_3]^+N_5^-$; (H) IR spectrum of volatiles from $(NH_3OH)^+N_5^-$; (I) IR spectrum of volatiles from $(NH_4)^+N_5^-$; and (J) IR spectrum of volatiles from $(N_2H_5)^+N_5^-$.

DOI: 10.1021/jacs.8b05106
J. Am. Chem. Soc. 2018, 140, 16488–16494

generated HN_3 gas[27] caused by heating, indicating that *cyclo*-N_5^- cannot undergo a single-step decomposition to N_2 bypassing N_3^- as an intermediate. The TG curves demonstrate that these pentazolate compounds exhibit good thermal stability with onset decomposition temperatures of more than 85 °C, except for $[N(CH_3)_4]^+N_5^-$ with an onset decomposition temperature of 80.8 °C, indicating that the cation-π interaction in $[N(CH_3)_4]^+N_5^-$ is weaker than the hydrogen bonding in the other pentazolate compounds. Their decomposition processes usually depend on the countercation and exhibit distinct weight losses in the temperature range of 40 °C to 300 °C. Both $[C(NH_2)_3]^+N_5^-$ and $[N(CH_3)_4]^+N_5^-$ underwent two pronounced rapid drastic weight losses, the first one involving the thermal decompositions of *cyclo*-N_5^- to N_3^- and the second one the thermal decompositions of the generated azides. These results are very similar to our previous findings for $(N_5)_6(H_3O)_3(NH_4)_4Cl$ and $[Co(H_2O)_4(N_5)_2]\cdot 4H_2O$.[11,12] The simultaneously recorded IR and MS spectra provide further evidence for their decomposition phases (Figures S27 and S28). However, we were most interested in $(NH_3OH)^+N_5^-$, $(NH_4)^+N_5^-$ and $(N_2H_5)^+N_5^-$. The thermal decomposition of these three compounds takes place in one rapid step between 90 and 125 °C with a mass loss of about 100%. The DSC curves show sharp exothermic peaks at 112 °C, 101 °C, and 100 °C for $(NH_3OH)^+N_5^-$, $(NH_4)^+N_5^-$, and $(N_2H_5)^+N_5^-$, respectively, which indicate extremely fast decomposition and energy releases within a small temperature range of 30 °C.

2.4. Spectral Properties. Nuclear magnetic resonance (NMR) studies can provide detailed structure information. In light of high nitrogen content of salts and their simple structures, the ^{15}N unlabeled pentazolate salts were investigated (Figures S12–S22). The ^{15}N NMR spectra of the *cyclo*-N_5^- salts exhibit a resonance in the −5.40 ppm to −4.98 ppm range except for $[N(CH_3)_4]^+N_5^-$ for which no signal was observed due to its weakness. These signals are in excellent agreement with the value of −6.5 ppm, predicted by Bartlett.[28] The natural abundance of ^{15}N signal in these salts show a unanimous chemical shift range of −5 ppm to −6 ppm for *cyclo*-N_5^-. The reliable ^{15}N NMR chemical shift determination for *cyclo*-N_5^- is also relevant with respect to the previous dispute between the Christe[29] and Butler groups.[30]

The pentagonal-planar *cyclo*-N_5^- anion possesses D_{5h} symmetry with $(3n - 6) = 9$ fundamental vibrations, classified as $A_1' + E_1' + 2\,E_2' + E_2''$. Since it has a center of symmetry, the infrared and Raman bands are mutually exclusive, with the A_1' and E_2' modes being Raman active, the E_1' mode being infrared active, and the E_2'' mode being inactive in both the Ra and IR (see Figure 5). Because the present study provided five high-quality data sets for *cyclo*-pentazolates with relatively simple well-characterized counterions, it offered an opportunity to extract the fundamental modes of D_{5h} *cyclo*-N_5^-. The experimental data together with the theoretical predictions[31] are summarized in Table 1 and show excellent agreement after subtraction of the known cation bands (Figures S2–S11). For the vibrational spectra of NH_4^+, $N(CH_3)_4^+$, $N_2H_5^+$, and NH_3OH^+ see the book by Siebert[32] and for the guanidinium cation the paper by Becker.[33] This provides further support for the presence of a highly symmetrical N_5^- anion, as shown by the crystal structures of these compounds.

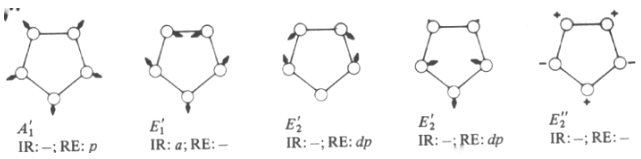

Figure 5. Normal modes for D_{5h} of *cyclo*-N_5^-.

The infrared spectrum of $(N_5)_6(H_3O)_3(NH_4)_4Cl$[11] was also recorded, and the presence of the *cyclo*-N_5^- anion was established by a sharp prominent band at 1224 cm^{-1}. Furthermore, Table 1 shows that the frequencies of the *cyclo*-N_5^- anion stretching modes in its tetramethylammonium salt are red-shifted by about 20 cm^{-1}, when compared to those of the remaining N_5^- salts. This shift can be attributed to the fact that the crystal structure of the $N(CH_3)_4^+$ salt significantly differs from those of the other salts, exhibiting C–H···π interactions.

2.5. Physical Properties. To evaluate the properties of the different *cyclo*-pentazolate salts, crystal densities, ^{15}N NMR chemical shifts, decomposition temperature onsets, energetic performances, and impact and friction sensitivities were evaluated and are summarized in Table 2. The densities of the five pentazolates are in the range 1.25–1.64 g/cm^3 and are significantly lower than those of the reported metal *cyclo*-pentazolates and *cg*-N (3.4355 g/cm^3) but are almost the same as that predicted for N_8.[8] The lower densities of the pentazolates of this study are mainly due to the smaller contributions from the cations to the overall density and the ambient pressure conditions, respectively.

The results of our performance calculations, given in Table 2 and all carried out with the Cheetah 7.0 program, show that the *cyclo*-N_5^- salts are energetic materials, outperforming the corresponding azides, and in the case of the hydrazinium and hydroxylammonium salts match the detonation pressure of RDX, but significantly exceed RDX and HMX in terms of detonation velocity due to their high energetic-nitrogen content. Although the ammonium salt has a lower detonation pressure than RDX, its detonation velocity also exceeds those of RDX and HMX. As rocket propellants, the hydrazinium compound shows a slightly higher and the hydroxyl ammonium compound a significantly higher sea-level specific impulse than RDX and HMX. As expected from the large nonenergetic cation, the tetramethylammonium salts are the lowest performers, followed by the guanidinium salts. The high performances of the hydrazinium and hydroxyl ammonium salts are not surprising. The hydroxyl ammonium cation contributes an oxygen atom to the combustion process, while hydrazine by itself is already a good rocket propellant. However, the thermal stabilities of these pentazolates are insufficient for practical applications as energetic materials.

3. CONCLUSIONS

The new *cyclo*-pentazolate salts containing the simple nitrogen-rich cations NH_4^+, NH_3OH^+, $N_2H_5^+$, $C(NH_2)_3^+$, and $N(CH_3)_4^+$ have been prepared by metathetical reactions. These salts were characterized by their crystal structures, vibrational, mass and multinuclear NMR spectra, thermal stability measurements, sensitivity data, and performance calculations. It is shown that *cyclo*-pentazolates are more energetic than the corresponding azides but are thermally less stable decomposing in the range of 80 °C to 105 °C. As explosives, the hydrazinium and hydroxyl ammonium salts are predicted to match the detonation pressure of RDX but exhibit significantly higher detonation velocities with comparable impact and

DOI: 10.1021/jacs.8b05106
J. Am. Chem. Soc. 2018, 140, 16488–16494

Table 1. Calculated and Observed Vibrational Spectra of *cyclo*-N_5^- in Space Group D_{5h}

mode descript. c-N_5^- in D_{5h}	calcd freq, cm^{-1} (intens)[a]		obsd freq, cm^{-1} (rel intens)[a] counterion				
	B3LYP/aug-cc-p-VDZ	CCSD(T)/aug-cc-pVDZ	NH_3OH^+	$C(NH_2)_3^+$	$N(CH_3)_4^+$	$N_2H_5^+$	NH_4^+
A_1' ν_1 (RA)	1189.7 [38.6]	1141 [47.8]	1187 vs	1176 vs	1153 vs	1170 vs	1176 vs
E_1' ν_2 (IR)	1243.7 (17.5)	1202 (13.6)	1222 vs	1221 vs	1202 m	1218 s	1221 s
E_2' ν_3 (RA)	1106.5 [0.3]	1078 [1.8]	1120 vw	1112 vw	[b]	1137 vw[d] 1105 vw[d]	1108 vw
ν_4 (RA)	1016.6 [2.4]	1001 [1.5]	1005 vw	1010[c]	1006 w	[e]	1020 vw
E_2'' ν_5 (ia)	769.5	739					

[a]Relative intensities, vs = very strong, s = strong, m = medium, w = weak, vw = very weak. [b]Not observed due to its very low intensity. [c]Band coincides with the very strong symmetric CN_3 stretching mode of the guanidinium skeleton; [d]Doubly degenerate E-mode, split into its degenerate components; [e]Band is hidden by the strong 976 cm^{-1} band of the $N_2H_5^+$ cation.

Table 2. Physical Properties of Five *cyclo*-Pentazolate Compounds and Three Azide Compounds and Their Comparison with RDX and HMX

comp.	d[a] ($g\ cm^{-3}$)	^{15}N NMR[b] (ppm)	T_d[c] (°C)	N[d] (%)	ΔH_f[e] ($kJ\ mol^{-1}$)	v_D[f] ($km\ s^{-1}$)	P[g] (GPa)	sea level Isp (sec)	IS[h] (J)	FS[i] (N)
$[N(CH_3)_4]^+N_5^-$	1.245	not obsd	80.8	58.29	297.2	5.88	10.08	197.7	35	>360
$[C(NH_2)_3]^+N_5^-$	1.515	−5.40	88.1	86.12	312.3	7.96	20.14	201.5	24	>360
$(NH_3OH)^+N_5^-$	1.636	−5.03	104.3	80.70	371.7	9.93	35.80	281.7	6	60
$(NH_4)^+N_5^-$	1.520	−4.98	102.0	95.42	308.1	9.28	27.29	238.0	13	140
$(N_2H_5)^+N_5^-$	1.620	−5.33	85.3	95.11	471.3	10.40	37.00	266.3	6	100
$[N(CH_3)_4]^+N_3^-$	1.156			48.28	222.3	5.50	8.10	200.7	insens	insens
$(NH_4)^+N_3^-$	1.346		400	93.33	112.1	8.81	21.70	242.7	>118	
$(N_2H_5)^+N_3^-$	1.40			93.33	383.4	9.63	27.85	282.2		
RDX[j]	1.816		230	37.84	70.03	8.84	35.84	259.8	7.4(7.5)[k]	120(120)[k]
HMX	1.905		277	37.84	75.03	9.16	41.18	258.8	7.4	120

[a]Crystal density from crystal structures. [b]Chemical shift for ^{15}N-unlabeled *cyclo*-N_5^-. [c]Temperature of decomposition by TG (5 °C/min, onset values). [d]Nitrogen content. [e]Heat of formation, all calculations for the *cyclo*-N_5^- salts were carried out by Dixon and Vasiliu with the G3MP2 method. [f]Detonation velocity. [g]Detonation pressure. [h]Impact sensitivity (this study). [i]Friction sensitivity (this study). [j]RDX and HMX values calculated with Cheetah 7.0. [k]This study.

friction sensitivities. As a rocket propellant, the hydrazinium salt is predicted to match the performance of RDX, while the hydroxyl ammonium salt significantly outperforms RDX. The crystal structures show that the *cyclo*-pentazolate anions are generally stabilized by hydrogen bonds to the cations, except for the $N(CH_3)_4^+$ salt which also exhibits strong cation-π interactions. For practical applications, ways must be found to further increase the thermal stability of the *cyclo*-pentazolate anion.

■ ASSOCIATED CONTENT

Supporting Information

The Supporting Information is available free of charge on the ACS Publications website at DOI: 10.1021/jacs.8b05106.

Experimental and characterization data; Figures S1−S41; and Tables S1−S29 (PDF)

X-ray crystallographic files (ZIP)

■ AUTHOR INFORMATION

Corresponding Authors

*hubc@njust.edu.cn

*sunyangguo2004@163.com

ORCID

Chao Jiang: 0000-0002-9228-1924

Jun Luo: 0000-0002-8093-5345

Bingcheng Hu: 0000-0002-0371-8128

Author Contributions

⊥C.Y. and C.Z. contributed equally to this work.

Notes

The authors declare no competing financial interest.

■ ACKNOWLEDGMENTS

The authors gratefully acknowledge the financial support provided by the Fundamental Research Funds for the Central Universities (No. 30917011101), the Priority Academic Program Development of jiangsu Higher Education Institutions (PAPD) and the National Natural Science Foundation of China (No. 21701077). The authors are most grateful to K.O.C. (University of Southern California) for his professional expertise to help rewriting the paper. All the theoretical calculation data in the paper are provided by K.O.C. We are also indebted to and thank K.O.C. and other members of our group for many helpful and inspired discussions and support of our work. The authors thank David Dixon (University of Alabama) and Monica Vasiliu (University of Alabama) for the calculation of the heats of formation. The authors also thank Yue Zhao (Nanjing University) and Fengfeng Wang (Institute of material medica, Chinese Academy of Medical Science & Peking Union Medical College) for expert crystallographic analysis.

■ REFERENCES

(1) Seth, S.; McDonald, K. A.; Matzger, A. *Inorg. Chem.* **2017**, *56*, 10151.

(2) Zhang, W. Q.; Zhang, J. H.; Deng, M. C.; Qi, X. J.; Nie, F. D.; Zhang, Q. H. *Nat. Commun.* **2017**, *8*, 181.

(3) Klapötke, T. M.; Sabaté, C. M. *Chem. Mater.* **2008**, *20*, 3629.

DOI: 10.1021/jacs.8b05106
J. Am. Chem. Soc. 2018, 140, 16488−16494

(4) Talawar, M. B.; Sivabalan, R.; Mukundan, T.; Muthurajan, H.; Sikder, A. K.; Gandhe, B. R.; Rao, A. S. *J. Hazard. Mater.* **2009**, *161*, 589.
(5) Yu, Q.; Yin, P.; Zhang, J. H.; He, C. L.; Imler, G. H.; Parrish, D. A.; Shreeve, J. M. *J. Am. Chem. Soc.* **2017**, *139*, 8816.
(6) Kumar, D.; Imler, G. H.; Parrish, D. A.; Shreeve, J. M. *Chem. - Eur. J.* **2017**, *23*, 7876.
(7) Christe, K. O.; Wilson, W. W.; Sheehy, J. A.; Boatz, J. A. *Angew. Chem., Int. Ed.* **1999**, *38*, 2004.
(8) Hirshberg, B.; Gerber, R. B.; Krylov, A. I. *Nat. Chem.* **2014**, *6*, 52.
(9) Olson, J. K.; Ivanov, A. S.; Boldyrev, A. I. *Chem. - Eur. J.* **2014**, *20*, 6636.
(10) (a) Christe, K. O. *Science* **2017**, *355*, 351. (b) Curtius, T. *Ber. Dtsch. Chem. Ges.* **1890**, *23*, 3023. (c) Bazanov, B.; Geiger, U.; Carmieli, R.; Grinstein, D.; Welner, S.; Haas, Y. *Angew. Chem., Int. Ed.* **2016**, *55*, 13233.
(11) Zhang, C.; Sun, C. G.; Hu, B. C.; Yu, C. M.; Lu, M. *Science* **2017**, *355*, 374.
(12) Zhang, C.; Yang, C.; Hu, B. C.; Yu, C. M.; Zheng, Z. S.; Sun, C. G. *Angew. Chem., Int. Ed.* **2017**, *56*, 4512.
(13) Xu, Y. G.; Wang, Q.; Shen, C.; Lin, Q. H.; Wang, P. C.; Lu, M. *Nature* **2017**, *549*, 78.
(14) Zhang, W. Q.; Wang, K. C.; Li, J. C.; Lin, Z. E.; Song, S. W.; Huang, S. L.; Liu, Y.; Nie, F. D.; Zhang, Q. H. *Angew. Chem.* **2018**, *130*, 2622.
(15) Sun, C. G.; Zhang, C.; Jiang, C.; Yang, C.; Du, Y.; Zhao, Y.; Hu, B. C.; Zheng, Z. S.; Christe, K. O. *Nat. Commun.* **2018**, *9*, 1269.
(16) Steele, B. A.; Stavrou, E.; Crowhurst, J. C.; Zaug, J. M.; Prakapenka, V. B.; Oleynik, I. I. *Chem. Mater.* **2017**, *29*, 735.
(17) Laniel, D.; Weck, G.; Gaiffe, G.; Garbarino, G.; Loubeyre, P. *J. Phys. Chem. Lett.* **2018**, *9*, 1600.
(18) Arhangelskis, M.; Katsenis, A. D.; Morris, A. J.; Friščić, T. *Chem. Sci.* **2018**, *9*, 3367.
(19) Steele, B. A.; Oleynik, I. I. *Chem. Phys. Lett.* **2016**, *643*, 21.
(20) Steele, B. A.; Oleynik, I. I. *J. Phys. Chem. A* **2017**, *121*, 1808.
(21) Dumitrescu, D.; Legrand, Y. M.; Dumitrascu, F.; Barboiu, M.; Lee, A. V. D. *Cryst. Growth Des.* **2012**, *12*, 4258.
(22) Suezawa, H.; Yoshida, T.; Hirota, M.; Takahashi, H.; Umezawa, Y.; Honda, K.; Nishio, M.; Tsuboyama, S. *J. Chem. Soc., Perkin Trans 2* **2001**, *11*, 2053.
(23) Taylor, R.; Kennard, O. *J. Am. Chem. Soc.* **1982**, *104*, 5063.
(24) Nepal, B.; Scheiner, S. *J. Phys. Chem. A* **2014**, *118*, 9575.
(25) Hay, B. P.; Custelcean, R. *Cryst. Growth Des.* **2009**, *9*, 2539.
(26) Frontera, A.; Gamez, P.; Mascal, M.; Mooibroek, T. J.; Reedijk, J. *Angew. Chem., Int. Ed.* **2011**, *50*, 9564.
(27) Dows, D. A.; Pimentel, G. C. *J. Chem. Phys.* **1955**, *23*, 1258.
(28) Perera, S. A.; Gregušová, A.; Bartlett, R. J. *J. Phys. Chem. A* **2009**, *113*, 3197.
(29) Schroer, T.; Haiges, R.; Schneider, S.; Christe, K. O. *Chem. Commun.* **2005**, *0*, 1607.
(30) Butler, R. N.; Hanniffy, J. M.; Stephens, J. C.; Burke, L. A. *J. Org. Chem.* **2008**, *73*, 1354.
(31) (a) Dixon, D. A.; Feller, D.; Christe, K. O.; Wilson, W. W.; Vij, A.; Vij, V.; Jenkins, H. D. B.; Olson, R. M.; Gordon, M. S. *J. Am. Chem. Soc.* **2004**, *126*, 834. (b) Bartlett, R. J. Structure and Stability of Polynitrogen Molecules and Their Spectroscopic Characteristics. *AFOSR-DARPA Report*, F49620-98-1-0477; University of Florida: Gainesville, FL.
(32) Siebert, H. *Anwedungen der Schwingungsspektroskopie in der Anorganischen Chemie, Anorganische und Allgemeine Chemie in Einzeldarstellungen, VII*; Springer Verlag: 1966.
(33) Němec, I.; Matulková, I.; Held, P.; Kroupa, J.; Němec, P.; Li, D. X.; Bohatý, L.; Becker, P. *Opt. Mater.* **2017**, *69*, 420.

DOI: 10.1021/jacs.8b05106
J. Am. Chem. Soc. 2018, 140, 16488−16494